nature physics
SUPPLEMENTARY INFORMATION
DOI: 10.1038/NPHYS1303

# Supplementary Information - Resolved-sideband and cryogenic cooling of an optomechanical resonator: Toward the quantum ground state

Young-Shin Park and Hailin Wang

Department of Physics and Oregon Center for Optics
University of Oregon, Eugene, Oregon 97403, USA

## 1) Fabrication of deformed microspheres

Deformed silica microspheres were fabricated by fusing together two regular microspheres of similar sizes with a focused $CO_2$ laser beam. Through repeated heating, we can control the degree of deformation, defined as $\varepsilon = r_a / r_b - 1$, where $r_a$ and $r_b$ are the radius for long and short axis, respectively. Figures 1a-1c show scanning electron micrograph (SEM) images of a deformed silica microsphere (with estimated deformation of 5%) obtained along three orthogonal directions.

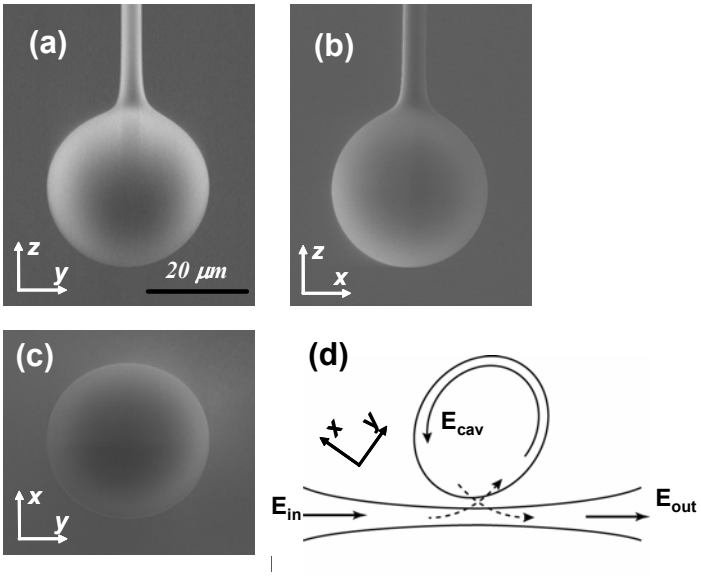


FIG 1. (a)-(c) SEM images of a deformed silica microsphere obtained along three orthogonal directions. (d) The geometry of free space evanescent excitation.

## 2) Free space excitation

For free space excitation of whispering gallery modes (WGMs), the silica microsphere is held in a vertical position (see Fig. 1a). The excitation laser beam is in the horizontal equatorial plane and is focused onto a region, which is 45 degrees away from a symmetry axis, as shown schematically in Fig. 1d. The behavior of free space evanescent excitation is similar to the well-known evanescent excitation of WGMs with a fiber taper except for two main differences. First of all, the free space excitation process does not lead to additional degradation of the optical *Q*-

DOI: 10.1038/NPHYS1303

factor. Secondly, the free space excitation efficiency is in part limited by the imperfect mode matching between the incident laser beam and the relevant WGM. In comparison, nearly perfect mode matching can be achieved with a fiber taper.

Figure 2a shows the transmission spectrum obtained near a WGM resonance for a silica microsphere with $d$=30 μm and deformation near 4%. The relative depth (or the fractional dip) of the transmission resonance depends sensitively on the position of the laser focal spot. Figure 2b shows the fractional dip of the WGM transmission resonance as a function of the distance between the laser spot and sphere surface. The maximum fractional dip observed exceeds 50%.

If we assume that the cavity loss is entirely due to output coupling along the four emission directions 45 degrees away from a symmetry axis [1], perfect mode matching between the incident laser beam and the relevant WGM should lead to a fractional dip of 75%. A mode matching coefficient (as defined in [2]) of 0.6 will lead to a fractional dip near 50%. For silica microspheres with smaller deformation, the fractional dip observed is considerably smaller. For these spheres, cavity losses other than those due to the output coupling become important.

For studies carried out at different bath temperatures, free space excitation is optimized at each temperature. Nearly the same optimal excitation efficiency can be achieved for temperatures ranging from 1.4 K to 300 K.

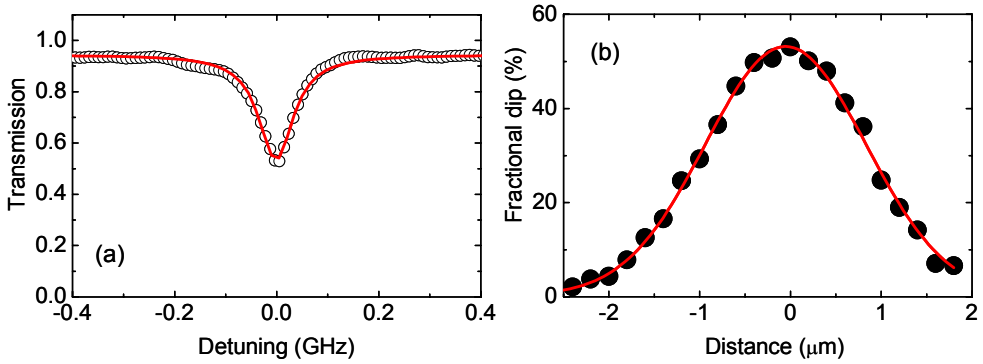


FIG 2. (a) Transmission spectrum (open circles) near a WGM resonance obtained with free space excitation. The solid curve is a Lorentzian fit. (b) Fractional dip (solid circles) obtained from the transmission spectrum as a function of the distance between the focused laser beam and the microsphere surface. The solid line is a Gaussian fit, showing a full width at half maximum of 1.8 μm. Note that we set the position of maximum fractional dip as the zero distance.

### 3) Excitation laser

For excitation of WGMs, we have used a tunable Ti:Sapphire ring laser near λ=800 nm (Coherent 899-21). The laser is frequency-stabilized to an external resonator and the laser linewidth is less than 0.5 MHz. Far above the lasing threshold, the spectral noise power measured near 100 MHz (after the subtraction of detector noise) is proportional to the attenuated laser power. This confirms that the laser intensity fluctuation near 100 MHz is shot-noise limited. The dependence of the intensity fluctuation on the attenuation provides a sensitive measure of excess intensity fluctuations above the shot noise limit since a large attenuation suppresses excess intensity fluctuations [3].

**4) Homodyne detection**

For simplicity, we have used the same laser beam for both resolved sideband cooling and homodyne detection of the mechanical vibration. In this configuration, the part of the incident laser beam, which is not coupled to the relevant WGM, provides a local oscillator for the homodyne interfereometric detection of the mechanical displacement. An AC-coupled photodiode (New Focus 1801) with a 3-dB bandwidth of 125 MHz is used for the homodyne detection.

For measurements of displacement power spectrum at room temperature, a single scan with 1 kHz resolution bandwidth is used. For studies carried out at cryogenic temperatures, 10 averages are taken per spectrum and a resolution bandwidth of 10 kHz is used. In these measurements, the laser shot noise far exceeds the detector noise when the laser power incident on the photodiode exceeds 1 mW.

Figure 3 shows the peak amplitude of the displacement power spectrum associated with the (*1, 0*) mechanical mode (after the subtraction of the noise floor) as a function of the detuning between the excitation laser and the WGM resonance. As shown in Fig. 3, the direct homodyne detection of mechanical displacement is the most sensitive when the laser frequency, $\omega/2\pi$ , is detuned by one mechanical frequency, $\omega_m/2\pi$, from the WGM frequency, $\omega_0/2\pi$. The direct homodyne detection is not effective at zero detuning, in contrast to the homodyne detection in the Hansch-Couillaud configuration [4]. Our experimental results are in good agreement with the theoretical calculation [5].

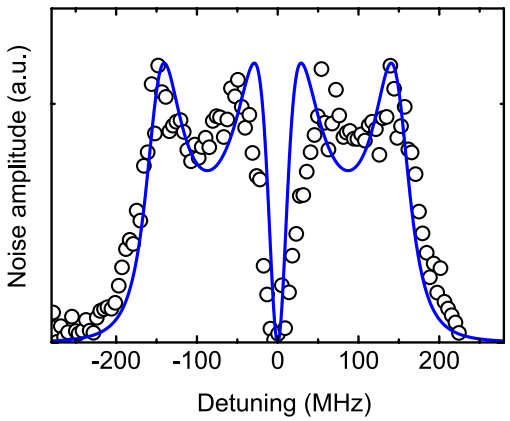


FIG 3. The peak amplitude of the spectral noise power of the (*1, 0*) mechanical mode (the open circles) as a function of the laser detuning. The experiment was carried out at room temperature with $\omega_m/2\pi$ =148.5MHz, $\kappa/2\pi$ =54MHz, $\lambda$ = 790nm, and $d$ = 30 μm. Optomechanically induced cooling or heating is negligible because of the weak excitation power (< 0.05 $P_{th}$). The solid curve shows the result of the theoretical calculation [5].

DOI: 10.1038/NPHYS1303

**5) Calibration of the mechanical displacement**

To calibrate the mechanical displacement measured from noise power spectrum, we modulate the phase of the excitation laser beam with an electro-optic modulator (EOM). This phase modulation mimics the phase shift induced by the mechanical oscillations. With the phase modulation, the incident optical field is described by

$$E_{in} \rightarrow E_{in} e^{i\beta \sin(\Omega_{ph} t)} \qquad \text{(S1)}$$

where $\beta$ and $\Omega_{ph}/2\pi$ are the amplitude and frequency of the phase modulation, respectively. For the direct homodyne detection and in the resolved sideband limit, a mechanical vibration with amplitude $r_0$ leads to the same signal as a phase modulation with amplitude $\beta = 2\omega_0 r_0 / \omega_m d$, where we have also assumed $\omega_m \approx \Omega_{ph}$ and $\omega - \omega_0 = \pm\omega_m$ [5]. Note that this result is the same as the homodyne detection with $\omega = \omega_0$ in the Hansch-Couillaud configuration [4].

Figure 4 shows the noise power spectrum obtained with a phase-modulated excitation laser beam. A resonance due to the phase modulation at $\Omega_{ph}/2\pi$=100.9 MHz appears along with the resonance associated with the (*1, 2*) mechanical mode. The modulation amplitude $\beta$ is obtained from a separate measurement of the relative intensity of the first sideband with the use of an optical spectrum analyzer. Note that the calibration is independent of the cavity decay rate, the mode matching efficiency, and the free space excitation efficiency. Using the equipartition theorem, we have also determined the effective mass of the mechanical mode, which is within 5% of the theoretical value calculated with finite element analysis.

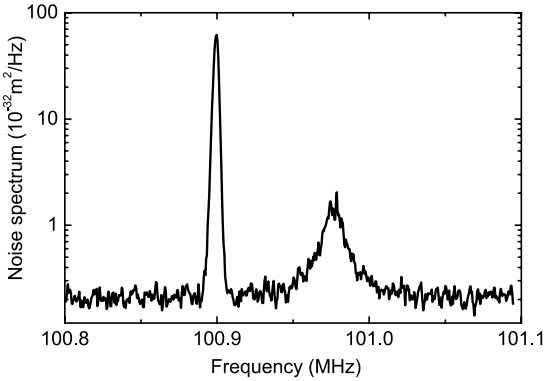


FIG 4. Calibration of the noise power spectrum. The phase of the excitation laser beam is modulated with an EOM with $\beta$ = 0.01 and $\Omega_{ph}/2\pi$ = 100.90 MHz. A radial amplitude of $r_0$ = 1.58 × $10^{-14}$ *m* and an effective mass of ~ 41 ± 1 *ng* are obtained for the (*1, 2*) mechanical mode with $\omega_m/2\pi$ = 100.98 MHz. The experiment was carried out at room temperature, with $\Delta\omega = -\omega_m$, and in a silica microsphere with $d$ = 31 μm and $\kappa/2\pi$ = 25 MHz.

**6) Error bars for phonon occupation**

We estimate an error bar better than 15% for the measured phonon occupation at low temperature. Half of this is due to uncertainties in determining the area of the mechanical resonance in the noise power spectrum and the other half is due to uncertainties in determining the bath temperature (plus or minus 0.1 K).

**Reference:**

1) Lacey, S., Wang, H., Foster, D. H., and Nockel, J. U. Directional tunneling escape from nearly spherical optical resonators. *Phys. Rev. Lett.* **91**, 033902 (2003).
2) Gorodetsky, M.L. and Ilchenko, V.S. Optical microsphere resonators: optimal coupling to high-Q whispering gallery modes. *J. Opt. Soc. Am. B* **16**, 147 (1999).
3) Yuen, H.P. and Chan, V.W.S. Noise in homodyne and heterodyne detection. *Opt. Lett.* **8**, 177 (1983).
4) Schliesser, A., Riviere, R., Anetsberger, G., Arcizet, O., and Kippenberg, T. J. Resolved-sideband cooling of a micromechanical oscillator. *Nature Physics* **4**, 415-419 (2008).
5) Park, Y.-S. and Wang, H. Unpublished.